Geophysical Journal International

Geophys. J. Int. (2020) **220,** 753–758 doi: 10.1093/gji/ggz463
GJI Gravity, Geodesy and Tides

Frequency dependence of the polar motion resonance

C. Bizouard, I. Nurul Huda, Y. Ziegler and S. Lambert

SYRTE, Observatoire de Paris, Université PSL, CNRS, Sorbonne Université, 77 av. Denfert-Rochereau, 75014 Paris, France. E-mail: christian.bizouard@obspm.fr

Accepted 2019 October 13. Received 2019 September 26; in original form 2019 March 7

SUMMARY

The nutation of the Celestial Intermediate Pole can be considered as a retrograde diurnal polar motion. As the common polar motion, it presents a resonance, but with period T_{PM} and quality factor Q_{PM} differing from the ones characterizing the Chandler wobble ($T_{\mathrm{CW}} =$ 430.2−431.6 d, Q_{CW} in the interval (56 255) according to Nastula & Gross): according to the nutation analysis presented in a separate paper, this period is about $T_{\mathrm{PM}} = 380$ d and the quality factor becomes −10. In this study, we aim to revisit the geophysical interpretation of this result. Two complementary factors account for the observed values: the non-equilibrium response of the ocean to the pole tide potential in the diurnal band, and the resonance of the solid Earth tide at the free core nutation period. This leads to a resonance of T_{PM} in the vicinity of the free core nutation period, confirmed by estimates derived from nutation analysis.

Key words: Elasticity and anelasticity; Core; Structure of the Earth; Earth rotation variations; Sea level change; Rheology: mantle.

1 INTRODUCTION

For a rigid Earth, of dynamic flattening e equal to the one of the real Earth, the terrestrial motion of the rotation pole, the so-called polar motion (PM), presents a free counterclockwise oscillation—the Euler wobble—with frequency $e\Omega$, where Ω is mean Earth angular velocity. The corresponding period is 304 d. But the observed polar motion presents a dominant broad band peak at the Chandler period $T_c = 430-432$ d. This lengthening from 304 to 432 d is commonly interpreted as the non rigid Earth response to the centrifugal potential variation caused by polar motion. The corresponding hydrostatic sea level change and elastic mantle deformation result in an inertia moment variation linearly dependent on the pole coordinates, modifying in turn the resonance frequency (Smith & Dahlen 1981). Moreover, dissipation in mantle accounts for a damping at this resonant period described by the quality factor $Q_{\mathrm{CW}} \sim 56-255$ (Nastula & Gross 2015). If we reasonably assume that the linear coefficients linking feedback inertia moments to polar displacement mostly rely on the static properties of the Earth, the resonance parameters should be the same at any timescales. As the excitation at stake is a random process in the spectral band surrounding T_{CW}, the Chandler wobble does not result from a single harmonic and its maximum can occur at a period slightly differing from the resonance frequency T_{CW}.

Meanwhile, in the decades 1960–1980 preceding the results obtained by the astrogeodetic VLBI, the achievement of the nutation theory for a quasi-elastic oceanless solid Earth containing a fluid core, led to formulate the effect of an additional resonance on the retrograde diurnal polar motion, reflecting the nutation terms in the non-rotating system: the free core nutation (FCN) resonance with the frequency $\sigma_{\mathrm{FCN}} = -1.005$ cycle/mean solar day (cpd). As the oceans were discarded from the theory, the common PM resonance appeared with the shortened period of $T_{\mathrm{PM}} = 401$ d whatever the earth model (Sasao & Wahr 1981, or 0.995 d for the corresponding retrograde diurnal nutation in the non-rotating frame). The extension of the Earth nutation theory to an axisymmetric three-layered Earth (considering the solid inner core) yielded a similar value (T_{PM} = 396 d), and led to two additional free modes, the free inner core nutation (FICN) and the inner core wobble (ICW), the observability of which is still an open issue (Mathews *et al.* 1991).

Since 2000, the shortening of T_{PM} in the diurnal band has been supported by the nutation observations. Indeed the lunisolar nutation terms, as estimated from VLBI processing, are related to the theoretical nutation terms for a rigid earth model through a frequency transfer function, determined by σ_{FCN} and the PM resonance complex frequency

$$\tilde{\sigma}_{\mathrm{PM}} = 2\pi/T_{\mathrm{PM}}\left(1 + \frac{i}{2Q_{\mathrm{PM}}}\right) = \sigma_{\mathrm{PM}} + i\alpha_{\mathrm{PM}}\,. \quad (1)$$

In the celestial system this angular frequency becomes $\tilde{\sigma}'_{\mathrm{PM}} = \tilde{\sigma}_{\mathrm{PM}} + \Omega$, where $\Omega = 7.292\,115 \times 10^{-5}$ rad s^{-1} is the mean Earth angular velocity. As lunisolar nutation components slightly resonate at σ_{PM}, the PM resonance parameters can be extracted from a set of observed and theoretical lunisolar nutation terms. The first estimates of this kind was done by Mathews *et al.* (2002) for the period 1980–2002, and they obtained $T_{\mathrm{PM}} = 383.5 \pm 1.5$ d, $1/(2T_{\mathrm{PM}}Q_{\mathrm{PM}})$ $= -0.0001361489(28)$ cycle/sidereal day according to table 3(a) of their paper. Equivalently the quality factor is $Q_{\mathrm{PM}} = -9.5 \pm 0.1$. Here Q_{PM} or the complex part α_{PM} of $\tilde{\sigma}_{\mathrm{PM}}$ does not characterize any dissipative processes, as in the case of the seasonal band: its negative value reflects the dynamic effect in the induced pole tide as it will be explained further, and does not have the common signification of a relative energy dissipation per cycle anyhow. Based upon a recent adjustment from VLBI observations covering the period 1984–2018 Nurul Huda *et al.* (2019) determined very close values: $T_{\mathrm{PM}} = 382 \pm 2$ d, $Q_{\mathrm{PM}} = -10 \pm 1$.

This hints a frequency dependence of the resonance period T_{PM}. In the retrograde diurnal band, the lengthening of T_{PM} should be mitigated by the response of the Earth. Mathews *et al.* (2002) advocated the dynamic ocean response to polar motion. An equilibrium pole tide tends to compensate the dynamic Earth ellipticity, making it more spherical, and lengthening subsequently T_{PM} by about 30 d. However, at diurnal frequency, the dynamic processes in the ocean take precedence, so that the induced pole tide is strongly phase-shifted with respect to the polar motion. In turn, the compensation of the Earth ellipticity is strongly mitigated, and T_{PM} gets closer to the Euler period of 303.4 d for a rigid Earth.

More generally, the frequency dependence of the Earth rheological properties has to be considered for modelling the polar motion in light of the precision wherewith it is determined. Chen *et al.* (2013a) had highlighted how the transfer function from the geophysical forcing to the common polar motion (periods beyond 2 d) is impacted by frequency dependence of the solid Earth anelasticity. In a complementary paper they concluded that such a modified transfer function could improve the reconstruction of the polar motion from the fluid layer excitation (Chen *et al.* 2013b). However, their modelling is still based upon fixed polar motion resonance parameters (T_{CW}, Q_{CW}). In contrast, our paper points out the modification that these parameters undergo at diurnal timescale. It provides a detailed account of this modification starting from the contemporaneous knowledge of the ocean response to the gravimetric diurnal tide. Then the free core nutation is shown to induce a strong frequency dependence of $\tilde{\sigma}_{\mathrm{PM}}$ even within the retrograde diurnal band. Finally, we discussed to which extent our theoretical estimates are confirmed by recent nutation determination of Nurul Huda *et al.* (2019).

2 RESONANT PERIOD OF THE COMMON POLAR MOTION

Let C be the Earth axial principal moment of inertia, A and A_{m} the equatorial principal moments of inertia of the Earth and of the mantle, respectively, $e = (C - A)/A \approx 1/304.5$ the Earth dynamic flattening and $\sigma_e = e\Omega$ the Euler frequency. The Earth rotation theory leads to the constant resonant angular frequency (Dehant & Mathews 2015)

$$\sigma_{\mathrm{PM}} = \sigma_e \frac{A}{A_{\mathrm{m}}} \left[1 - \frac{\tilde{k}}{k_s} + O(e) \right] , \tag{2}$$

where $k_s = 0.938$ is the secular Love number, and $\tilde{k} \approx 0.355$ a coefficient accounting for Earth response to the pole tide potential. Note that many studies favor the compliance $\kappa = e\tilde{k}/k_s$ instead of $\tilde{k}$. In the resonance frequency it clearly quantifies the compensation of the permanent rotational response—namely the ellipticity, e—by the variable instantaneous Earth rotational response :

$$\sigma_{\mathrm{PM}} = \frac{A}{A_{\mathrm{m}}} \Omega \left[e - \kappa + O(e^2) \right] . \tag{3}$$

Actually $\tilde{k}$ is composed of two parts:

$$\tilde{k} = \tilde{k}_2 + \tilde{k}_o . \tag{4}$$

Here $\tilde{k}_2$ is the body Love number of degree 2 accounting for the solid Earth response to the pole tide potential, and $\tilde{k}_o$ is the oceanic Love number describing the ocean response to the same potential. They determine the variation of off-diagonal moment of inertia $\tilde{c} = c_{13} + i c_{23}$ resulting from the ocean and solid pole tide deformation: $c = \tilde{k}/k_s(C - A)m$, where m means the complex coordinate of the polar motion.

For the common polar motion, which unfolds beyond 2 d, the ocean response is considered at equilibrium. This leads to $\tilde{k}_o = 0.0477$. The solid Earth response is assumed quasi-elastic, described by the body Love number $\tilde{k}_2 = 0.307 - i\, 0.0035$ (Petit & Luzum 2010). These values determine the resonance parameters ($T_{\mathrm{PM}} = 433.6$, $Q_{PM} = 85$), which are in conformity with the estimates obtained by fitting the observed polar motion to the hydro-atmospheric excitation. One of the most recent estimation of this kind is the one of (Nastula & Gross 2015), mentioned above, and yielding the 95 per cent confidence intervals (430 432) d for T_{PM} and (56 255) for Q_{PM}. Such a loose constraint for the quality factor stems from the uncertainty affecting the excitation in the seasonal band.

3 CONTRIBUTION OF THE DYNAMIC OCEAN RESPONSE

The possibility of dynamic effects in ocean pole tide was considered in the late 1980s in Dickman (1990) and Dickman (1988). This author concluded that the dynamic effects at seasonal scales lengthens the Chandler period by 1 d. Equivalently the oceanic Love number is increased by about 0.0014. Moreover, the dynamic processes slightly delay the ocean tide response: with a time damping of about 500–700 yr, much longer than the Chandler relaxation time (30 yr), the damping introduced an imaginary part in the Love number of about -2×10^{-4}. So, the hydrostatic pole tide remains an excellent approximation when considering the common polar motion. However, below 10 d, many studies have shown that the ocean response to an atmospheric pressure variation strongly departs from the equilibrium, so the hydrostatic pole tide is not sound and k_o should change accordingly. In the diurnal band, this issue can be solved in light of the diurnal ocean tides. For, as the pole tide potential has the same form than the lunisolar tesseral potential and is relevant to the same frequency band, the Earth response should be formally the same. It is well known that the diurnal ocean tides are strongly affected by dynamic processes. Currents are generated, and in turn a relative angular momentum. Meanwhile, the observed diurnal ocean tide height is smaller than the theoretical equilibrium tide produced by the tesseral lunisolar potential, and strongly out-of-phased with respect to it. Tidal component at frequency σ causes the equatorial oceanic angular momentum

$$\begin{aligned} lH(t) &= H_1 \cos(\theta(\sigma) + \chi - \Phi_1) + i\, H_2 \cos(\theta(\sigma) + \chi - \Phi_2) \\ h(t) &= h_1 \cos(\theta(\sigma) + \chi - \phi_1) + i\, h_2 \cos(\theta(\sigma) + \chi - \phi_2), \end{aligned} \tag{5}$$

where $\theta(\sigma)$ is the tidal argument, $H(t)$ and associated coefficients H_1, H_2, Φ_1, Φ_2 hold for the matter term and $h(t)$, and associated coefficients h_1, h_2, ϕ_1, ϕ_2 describe the current term. According to the FES 2012 ocean tidal model, the main diurnal constituents are for tesseral tides J_1, K_1, P_1, O_1, Q1. The corresponding coefficients calculated in Madzak (2016) are provided in Table 1. An ancient ocean tide model going back to 1996 yielded close estimates, as reported in Chao *et al.* (1996). For a given tidal constituent, the

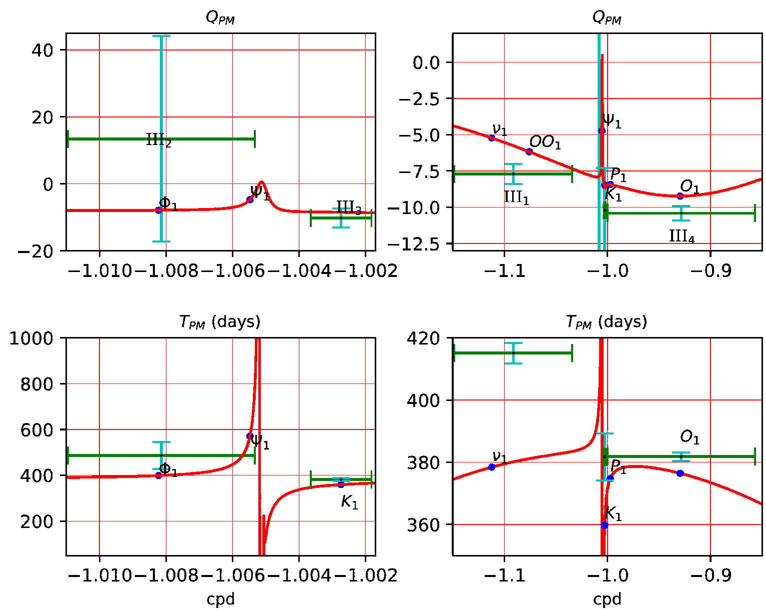

Figure 1. Resonance parameters of the polar motion in the diurnal retrograde band for an anelastic solid Earth covered by oceans. The blue points correspond to the five discrete tidal lines for which $k_{\rm o}$ values is deduced from FES 2012 ocean tidal model, as reported in Table 1. The continuous red line is associated with the $k_{\rm o}$ values obtained by a degree 2 polynomial fit.

Table 1. Main terms of the oceanic angular momentum generated by tesseral diurnal gravitational tides according to FES 2012, as reported in table 5.4 of Madzak (2016). Reported coefficient correspond to expression (5). The amplitudes H_1, H_2, h_1, h_2 are expressed in unit of 10^{25} kg m^2 s^{-1}, and $\gamma = GMST + \pi$.

	Tidal argument, θ	χ (°)	H_1	Φ_1 (°)	H_2	Φ_2 (°)	h_1	ϕ_1 (°)	h_2	ϕ_2 (°)
Q_1	$\gamma - l - 2F - 2\mathcal{N}$	−90	0.116	340.4	0.264	215.4	0.058	307.8	0.075	217.1
O_1	$\gamma - 2F - 2\mathcal{N}$	−90	0.476	330.1	1.178	221.9	0.291	299.7	0.442	206.1
P_1	$\gamma - 2F + 2D - 2\mathcal{N}$	−90	0.169	310.6	0.450	223.2	0.183	287.4	0.255	192.8
K_1	γ	+90	0.462	308.3	1.377	224.2	0.557	288.8	0.774	192.1
J_1	$\gamma + l$	+90	0.026	294.0	0.076	228.8	0.036	292.0	0.055	186.7

Table 2. Oceanic Love number in the diurnal band computed from FES 2012 ocean tidal model and tide generating potential according to (11).

Q_1	$-0.037 + i\,0.039$
O_1	$-0.030 + i\,0.038$
P_1	$-0.023 + i\,0.042$
K_1	$-0.023 + i\,0.042$
J_1	$-0.022 + i\,0.047$

retrograde term is

$$H^-(t) = (H^- + h^-)e^{-i(\theta+\chi)} \tag{6}$$

with

$$H^- = \left(\frac{H_1\cos(\Phi_1) - H_2\sin(\Phi_2)}{2} + i\,\frac{H_1\sin(\Phi_1) + H_2\cos(\Phi_2)}{2}\right)$$
$$h^- = \left(\frac{h_1\cos(\phi_1) - h_2\sin(\phi_2)}{2} + i\,\frac{h_1\sin(\phi_1) + h_2\cos(\phi_2)}{2}\right). \tag{7}$$

From (A4) and (A5), the corresponding tesseral lunisolar potential is $-\Omega^2 R_e^2/3Re\left(\tilde{\phi}(t)\mathcal{Y}_2^{-1}\right)$, with

$$\tilde{\phi}(t) = \frac{3gN_2^1}{\Omega^2 R_e^2}\xi_\sigma e^{-i(\theta_\sigma - \pi/2)}, \tag{8}$$

where ξ_σ is the equilibrium tidal height. Accounting for the deformation effect of the tidal loading, the retrograde effective angular momentum function caused by $\tilde{\phi}(t)$ is

$$\chi_o(t) = \frac{H^-(t)(1+k_2') + h^-(t)}{(C-A)\Omega} = \frac{H^-(1+k_2') + h^-}{(C-A)\Omega}e^{-i(\theta+\chi)}. \tag{9}$$

In the tidal potential W, expressed through (A4), $\tilde{\phi}(t)$ is formally equivalent to $m(t)$ in pole tide potential. So, $\chi_o(t)$ is proportional to $\tilde{\phi}(t)$, as the rotational excitation is proportional to $m(t)$:

$$\chi_o = \frac{\tilde{k}_o}{k_s}\tilde{\phi}, \tag{10}$$

where k_o is the oceanic Love number. Then, we obtain

$$\tilde{k}_o = k_s\frac{H^-(t)(1+k_2') + h^-(t)}{(C-A)\Omega\tilde{\Phi}} = -k_s\frac{H^-(1+k_2') + h^-}{C-A}\frac{\Omega R_e^2}{3gN_2^1\xi_\sigma}. \tag{11}$$

Then we can estimate $\tilde{k}_o$ for the tidal components here-above by considering the ξ_σ values reported in Table A1 of the Appendix. The resonance of the loading love number k_2' at FCN frequency

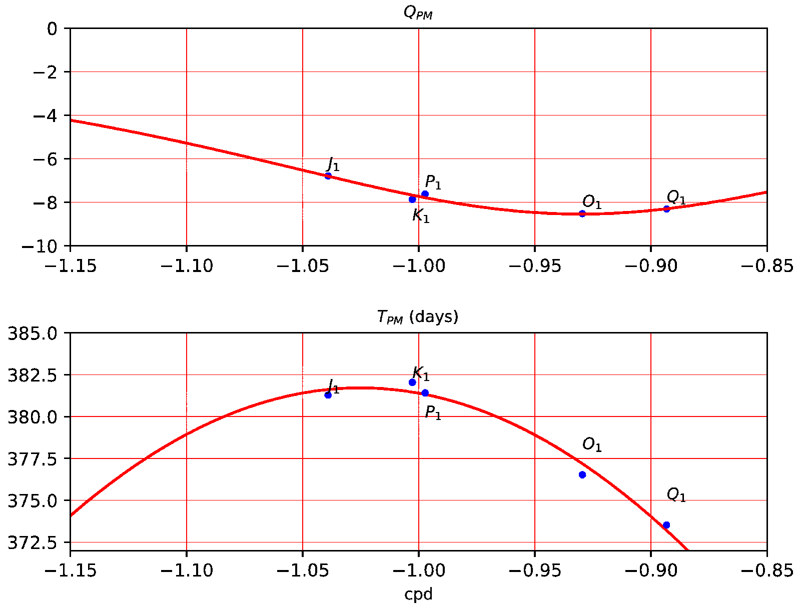

Figure 2. Resonance parameters of the polar motion in the diurnal retrograde band for an anelastic Earth covered by oceans and containing a fluid core. Green crosses specify the values obtained from nutation inversion over the restricted frequency bands III_1 (ν_1,OO_1), III_2 (Φ_1, Ψ_1), III_3 (K_1) and III_4 (S_1,P_1,O_1,Q_1): the horizontal bar extension gives the frequency band, and the vertical bar the uncertainty of the estimated value.

Table 3. Parameters of the polar motion resonance as determined from observed nutation inversion over different frequency bands (Nurul Huda *et al.* 2019).

Band	Frequency (cpd)	P_{PM}	Q_{PM}
I	$(-\Omega - 1/6.86 \le \sigma \le -\Omega + 1/6.86)$	382.0 ± 1.3	-10.4 ± 0.5
II_1	$(-\Omega - 1/6.86 \le \sigma \le -\Omega - 1/386)$	418.5 ± 7.2	-8.24 ± 1.7
II_2	$(-\Omega - 1/1095.18 \le \sigma \le -\Omega + 1/6.86)$	381.8 ± 1.2	-10.4 ± 0.5
III_1	$(-\Omega - 1/6.86 \le \sigma \le -\Omega - 1/31.81)$	415.1 ± 3.3	-7.7 ± 0.7
III_2	$(-\Omega - 1/121.75 \le \sigma \le -\Omega - 1/386)$	486.8 ± 58.4	13.4 ± 30.7
III_3	$(-\Omega - 1/1095.18 \le \sigma \le -\Omega + 1/1095.18)$	381.7 ± 7.6	-10.2 ± 2.9
III_4	$(-\Omega + 1/386 \le \sigma \le -\Omega + 1/6.86)$	381.8 ± 1.3	-10.4 ± 0.5

does not impact significantly $\tilde{k}_o$ in the retrograde diurnal band. For $k_2' = -0.3075$, the obtained values are given in Table 2. They differ strikingly from the oceanic Love number $k_o = 0.0477$ estimated for an equilibrium pole tide. These results can be compared with the estimate of Mathews *et al.* (2002) for K_1 tide. In term of compliance we have $\tilde{\kappa}_o = \tilde{k}_o e/k_s = (-7.9 + i\ 14.6)\ 10^{-5}$ in agreement with $(-6.9 + i\ 11.5)\ 10^{-5}$, as estimated in appendix D of Mathews *et al.* (2002). The values of Table 2 allow to model $k_o(\sigma)$ through a degree 2 polynomial of the frequency:

$$k_o(f) = (-0.716 + i\,0.721) f^2 + (-1.483 + i\,1.337) f + (-0.791 + i\,0.658)\ , \tag{12}$$

where f is in cpd. This expression of k_o only holds for the diurnal domain. Then we see that the resonance frequency (2) becomes frequency dependent:

$$\sigma_{PM}(\sigma) = \sigma_e \frac{A}{A_m} \frac{\tilde{k}_2 + \tilde{k}_o(\sigma)}{k_s}\ , \tag{13}$$

where $\tilde{k}_2$ is taken as the Love number of an anelastic Earth. It slightly varies with frequency. In the diurnal domain we have $\tilde{k}_2 = 0.299 - i\ 0.00144$ in the diurnal band according to Petit & Luzum (2010). The associated period and quality factor, namely

$$T_{PM}(\sigma) = \frac{2\pi}{\mathrm{Re}(\sigma_{PM})}\ ,\quad Q_{PM}(\sigma) = \frac{\mathrm{Re}(\sigma_{PM})}{2\,\mathrm{Im}(\sigma_{PM})}\ , \tag{14}$$

are displayed in Fig. 1. So, in the frequency band [−1.15 cpd, −0.85 cpd], the dynamic ocean response leads to the resonance parameters lying in the intervals ($374\ \mathrm{d} < T_{PM} \le 382.5\ \mathrm{d}$, $-5 \le Q_{PM} \le -10$). These theoretical estimates are confirmed by the analysis of lunisolar nutation components done in Nurul Huda *et al.* (2019). The fit based upon the 42 principal nutation terms between 7 d and 18.6 yr (i.e. between frequencies −1.14 cpd and −0.85 cpd in the Earth) yields $T_{PM} = 382.0 \pm 1.3$ d and $Q_{PM} = -10.4 \pm 0.5$.

4 INFLUENCE OF THE FLUID CORE

In the diurnal band, close to the free core nutation diurnal period, the solid Earth tide departs from the one of a quasi-elastic Earth. Indeed, the induced tilt of the core with respect to the mantle modifies the Earth mass distribution and in turn surface gravity. Modelled in the 1960s, this phenomenon has been confirmed from the 1990s through the superconducting gravimeter measurements (Crossley 1997). Other perturbations, of much lesser amplitude (100 times less), occur because of the free inner core nutation (FICN) mode at $\sigma_{FICN} \sim 1.0017$ cpd in the TRF, and because of the Polar motion resonance appearing at the period of about 380 d, as justified in the former section.

From IERS Conventions 2010 (Petit & Luzum 2010, table 6.4, eqs 6.9 and 6.10), the perturbation of diurnal tide on geopotential can be described through the 'diurnal' Love number

$$k_2(\sigma) = 0.29954 - i\,0.1412 \times 10^{-2} - \frac{L_{\rm PM}}{\sigma - \sigma_{\rm PM}} - \frac{L_{\rm FCN}}{\sigma - \sigma_{\rm FCN}} - \frac{L_{\rm FICN}}{\sigma - \sigma_{\rm FICN}}\,, \tag{15}$$

with the quantities

$$\begin{aligned} L_{\rm PM} &= (-0.77896 \times 10^{-3} - i\,0.3711 \times 10^{-4})k \\ \sigma_{\rm PM} &= 0.0026081 - i\,0.0001365 \\ L_{\rm FCN} &= (0.90963 \times 10^{-4} - i\,0.2963 \times 10^{-5})k \\ \sigma_{\rm FCN} &= -(1.0050624 - i\,2.5 \times 10^{-5}) \\ L_{\rm FICN} &= (-0.11416 \times 10^{-5} + i\,0.5325 \times 10^{-7})k \\ \sigma_{\rm FICN} &= -(1.0017612 - i\,0.0007821)\,. \end{aligned} \tag{16}$$

expressed in cycle per solar day. Here $k = 1.002737811$ is the factor for converting solar day in sidereal day, and $\sigma_{\rm PM} \approx 1/383$ cpd.

Replacing in (13) the pure anelastic value of k_2 by its resonant version (15), we get

$$\sigma_{\rm PM}(\sigma) = \sigma_e \frac{A}{A_{\rm m}} \frac{\tilde{k}_2(\sigma) + \tilde{k}_o(\sigma)}{k_s}\,. \tag{17}$$

The resonance parameters deduced from (14) are plotted in Fig. 2 over the frequency band [−1.15 cpd,−0.85 cpd] (denoted band I). This theoretical curve is compared with the estimated values from different sets of dominant lunisolar nutation terms, as reported in Nurul Huda *et al.* (2019). In average, far from the resonance at $\sigma_{\rm FCN} = -1.005$ cpd, the theoretical curve grossly corresponds to the estimated value obtained for the whole band I ($T_{\rm PM} = 382 \pm 1.3$ d, $Q_{\rm PM} = -10 \pm 1$, see Table 3).

The resonance produced by the free core nutation strongly affects the tidal lines surrounding K$_1$—pertaining to the precession and the long period nutation terms (6798 d, 1095 d, 3399 d) in the CRF (band III$_3$)—and tidal lines close to Ψ_1—retrograde nutation terms in 365.25 d, 386 d in the CRF (band III$_2$). Can we detect this modification? Estimated value of $T_{\rm PM}$ from the nutation terms in the band III$_2$ ($T_{\rm PM} = 487 \pm 58$ d) confirms the enhancement of the resonance period around Ψ_1 (theoretical value of 470 d at Ψ_1). As well, the nutation inversion in the band III$_3$ partly supports the theoretical decrease around K_1 (estimated value $T_{\rm PM} = 382 \pm 8$ d versus modelled value $T_{\rm PM} \sim 360$ d). Meanwhile, the nutation inversion allows to get the modelled quality factor of the band K_1 (−10 versus −8.5). For the band Ψ_1 the interval of the estimated value ($Q_{\rm PM} = 13 \pm 31$) is too loose for confirming the modelled value (−5), but it can include the modelled quality factor at the side frequency $\sigma_{\rm FCN} = 1.005$ cpd (∼0).

Outside the narrow band of the free core nutation frequency, far from K_1 and Ψ_1, the resonance parameters rejoin the curves obtained for an anelastic Earth covered by oceans. At the right part of the spectrum corresponding to band III$_4$, covering tidal lines S_1 and O_1, the estimates ($T_{\rm PM} = 381.8 \pm 1.3$ d, $Q_{\rm PM} = -10.4 \pm 0.5$) slightly differ from the modelled parameters. For the opposite band (III$_1$), the estimated period increases up to 415 d, as expected from the resonance.

Whereas $T_{\rm PM}$ strikingly varies in the narrow band of the FCN, even sweeping retrograde diurnal periods, this does not produce any significant resonant effect. Indeed at $\sigma_{\rm FCN}$ the quality factor of the PM resonance is close to 0, associated with a very strong damping.

5 CONCLUSION

This frequency dependence of the Earth rheology leads to striking modification of polar motion resonance parameters in the retrograde diurnal band. The dynamic response of the oceans to the pole tide potential is the main factor reducing the polar motion period to about 380 d. The associated quality factor of about −10 reflects the strong phase-shift of this response with respect to the pole tide. These estimates confirm the crude modelling proposed in Mathews *et al.* (2002), who restrict their consideration to the K_1 band (associated with a lower bound for $T_{\rm PM}$ according to our study). Due to the free core nutation resonance, the body Love number strongly deviates from its mean value of 0.3 in vicinity of the FCN frequency ($\sigma_{\rm FCN} = -1.0050$ cpd). In turn, in the band [−1.15 cpd, −0.85 cpd] as observed from the Earth, the resonance period of the polar motion increases above 400 d for frequencies smaller than $\sigma_{\rm FCN}$, and remains below this threshold for the band above $\sigma_{\rm FCN}$. Moreover, in the band close to Ψ_1 tidal line, the Earth response presents an even stronger phase-shift, given a quality factor getting closer to 0. This should impact the transfer function between the rigid Earth nutation terms and the real ones, as determined from VLBI observations.

In contrast to common polar motion, the excitation at stake, namely the diurnal tidal torque through rigid Earth nutation terms, is almost perfectly known. Despite the remoteness of the polar resonance period from the retrograde diurnal nutation terms in the terrestrial frame, the confrontation of observed nutation terms to those of a rigid Earth, as carried out in Nurul Huda *et al.* (2019), amazingly confirms the modelled frequency dependence and FCN resonance of the body Love number. So, the lunisolar nutations determined by VLBI reflect the dynamic behavior of the ocean and the influence of the fluid core on solid Earth deformation in the retrograde diurnal band. Inversely it can be used to better constrain our knowledge of the Earth deformation at this timescale. Future investigations have to extend the frequency profile of the polar motion resonance to prograde diurnal, semi-diurnal and rapid variations of the polar motion, for which dynamics of the oceans cannot be discarded.

REFERENCES

Chao, B., Ray, R., Gipson, J., Egbert, G. & Ma, C., 1996. Diurnal/semidiurnal polar motion excited by oceanic tidal angular momentum, *J. geophys. Res.,* **101**(B9), 20 151–20 163.

Chen, W., Ray, J., Li, J., Huang, C. & Shen, W., 2013a. Polar motion excitations for an earth model with frequency-dependent responses: 1. A refined theory with insight into the earth's rheology and core-mantle coupling, *J. geophys. Res.,* **118,** 4975–4994.

Chen, W., Ray, J., Shen, W. & Huang, C., 2013b. Polar motion excitations for an earth model with frequency-dependent responses: 2. Numerical tests of the meteorological excitations, *J. geophys. Res.,* **118,** 4995–5007.

Crossley, D., 1997. *Earth's Deep Interior,* Gordon and Breach Sci. Publ.

Dehant, V. & Mathews, P. M., 2015. *Precession, Nutation and Wobble of the Earth,* Cambridge Univ. Press.

Dickman, S., 1988. The self consistent dynamic pole tide in non-global ocean, *Geophys. J.,* **94,** 519–543.

Dickman, S., 1990. The pole tide in deep oceans, *Geophys. Monogr. Ser.,* **59,** 59–67.

Madzak, M., 2016. Short period ocean tidal variations in Earth rotation, *PhD thesis*, TU Wien.

Mathews, P., Buffett, B., Herring, T. & Shapiro, I., 1991. Forced nutations of the earth: influence of inner core dynamics 2. numerical results and comparisons, *J. geophys. Res.,* **96**(B5), 8243–8257.

Mathews, P., Herring, T. & Buffett, B., 2002. Modeling of nutation and precession: new nutation series from non rigid earth and insights into the earth interior, *J. geophys. Res.,* **107**(B4), ETG 3–1-ETG 3-26.

Nastula, J. & Gross, R., 2015. Chandler wobble parameters from SLR and GRACE, *J. geophys. Res.,* **120,** 4474–4483.

Nurul Huda, I., Ziegler, Y., Bizouard, C. & Lambert, S., 2019. Nutation terms adjustment and implication for the earth rotation resonance parameters, *Geophys J. Int,* accepted.

Petit, G. & Luzum, B.E., 2010. IERS conventions 2010, BKG, Tech. rep.

Sasao, T. & Wahr, J., 1981. An excitation mechanism for the free core nutation, *Geophys. J. R. astr. Soc.,* **64,** 729–746.

Smith, M. & Dahlen, F., 1981. The period and q of the chandler wobble, *Geophys. J. R. astr. Soc,* **64,** 223–281.

APPENDIX: TESSERAL TIDAL POTENTIAL

The material of this appendix is inspired from Dehant & Mathews (2015, section 5.5). Consider a point of the Earth at distance r from the geocentre of latitude ϕ and longitude λ. At this place the tesseral part of the tidal potential generated by a celestial body of mass M—located in the true equatorial frame by its right ascension α, declination δ, and distance d from the geocentre—is given by

$$W = \frac{GM}{d^5}\frac{1}{3}d^2 P_2^1(\sin\delta) r^2 P_2^1(\sin\phi)\cos(\lambda-\alpha)\ . \tag{A1}$$

Here the polar motion effect on the tidal potential is neglected: astronomical and geographic latitudes are merged, as well as the node of prime meridian with the Terrestrial International Origin (Petit & Luzum 2010). Introducing the terrestrial Cartesian coordinates (x, y, z) and (d_x, d_y, d_z) of the location and of the celestial body respectively, we can easily derive

$$W = \frac{3GM}{d^5} z d_z \operatorname{Re}\left[(d_x + i d_y)(x - iy)\right]\ , \tag{A2}$$

Then, noting that $r^2\mathcal{Y}_2^{-1} = 3(xz - iyz)$, where $\mathcal{Y}_2^{-1} = 3\sin\theta\cos\theta e^{-i\lambda}$ is the complex conjugate of the non-normalized spherical harmonic function of degree 2 and order 1, we obtain

$$W = \frac{GM}{d^5} d_z r^2 \operatorname{Re}\left[(d_x + i d_y)\mathcal{Y}_2^{-1}\right]\ . \tag{A3}$$

It is useful to put the W into the form of the pole tide potential $\Delta U^{(r)} = -\frac{\Omega^2 r^2}{3}\operatorname{Re}\left[m(t)\mathcal{Y}_2^{-1}\right]$:

$$W = -\frac{\Omega^2 r^2}{3}\operatorname{Re}\left[\tilde{\phi}(t)\mathcal{Y}_2^{-1}\right],\ \text{with}\ \tilde{\phi}(t) = -\frac{3GM}{\Omega^2 d^5} d_z(d_x + i d_y). \tag{A4}$$

Then, $\tilde{\phi}(t)$, directly comparable to the polar motion m, presents the Cartwright–Taylor like expansion

$$\tilde{\phi}(t) = \frac{3gN_2^1}{\Omega^2 R_e^2}\sum_{\sigma\geq 0}\xi_\sigma e^{-i(\theta_\sigma(t)-\pi/2)}\ , \tag{A5}$$

where θ_σ is the tidal argument and σ the corresponding frequency. In Table A1, we report the coefficients of the tesseral lunisolar tides that are considered in this paper. For a given tidal component, the numerical application yields

Table A1. Coefficients of the lunisolar tides used in this paper, as reported in Dehant & Mathews (2015).

	σ (cpd)	$\theta_\sigma(t)$	ξ_σ (m)
Q_1		$GMST + \pi - l - 2F - 2\mathcal{N}$	−0.05021
O_1	0.9295	$GMST + \pi - 2F - 2\mathcal{N}$	−0.26223
P_1		$GMST + \pi - 2F + 2D - 2\mathcal{N}$	−0.12199
K_1	1.00273	$GMST + \pi$	0.36864
J_1		$GMST + \pi + l$	0.02062

$$\tilde{\phi}_\sigma(t) = 3.51\ 10^{-5}\,[\mathrm{m}^{-1}]\,\xi_\sigma\,[\mathrm{m}]e^{-i(\theta_\sigma(t)-\pi/2)}\ . \tag{A6}$$